Full Paper

Electrocatalytic Oxidation of Formaldehyde on PtPd Alloy Nanoparticle –Multi-Walled Carbon Nanotube–Ionic Liquid Composite Film

Lifeng Yang, Faqiong Zhao, Fei Xiao, Baizhao Zeng*

College of Chemistry and Molecular Sciences, Wuhan University, Wuhan 430072, P R China

* Corresponding Author; Tel: +86-27-68756626*;* Fax: 86-27-68754067

E-Mail: bzzeng@whu.edu.cn

Abstract- PtPd alloy nanoparticles were electrodeposited on a multi-walled carbon nanotube (MWNT)–ionic liquid (IL, i.e., 1-octyl-3-methylimidazolium hexafluophosphate, $OMIMPF_6$) composite film coated glassy carbon electrode. The resulting electrode (PtPd–MWNT–IL/GCE) was characterized by X-ray diffraction, scanning electron microscope and voltammetry. The influence of some parameters (e.g. electrodeposition time, electrodeposition potential and temperature) on the PtPd alloy nanoparticles was discussed and optimized. The electrocatalytic oxidation of formaldehyde on the electrode was explored, and it was found that the PtPd–MWNT–IL/GCE showed good electrochemical catalysis in H_2SO_4 solution. When the PtPd–MWNT–IL/GCE was used as a formaldehyde sensor, it displayed wide linear range and good stability.

Keywords- Platinum–Palladium Alloy Nanoparticles, Ionic Liquid, Multi-Walled Carbon Nanotubes, Formaldehyde, Electrocatalysis

1. INTRODUCTION

Metal platinum is usually used to prepare electro-catalysts as it has good catalytic activity to some electrochemical reactions, but pure platinum catalyst is easily poisoned by some species such as CO [1]. To improve the performance and reduce the expense of Pt catalyst, Pt-based alloy catalysts were developed. For example, PtPd, PtAu, PtNi alloy catalysts

showed better property than pure Pt catalyst [2-5]. As for this, several interpretations were proposed [3].

The performance of Pt-based catalysts is also related to the support, because the catalysts generally interact with the support [4,5]. In recent years, carbon nanotubes (CNTs) were widely used as catalyst support in electrochemical field [6,7] because they have high accessible surface area, low resistance and high chemical stability. Metallic catalyst particles could be decorated on the wall of CNTs [8]. In addition, ILs is useful in the synthesis of nanostructure and the immobilization of CNTs [9]. Therefore, the combination of CNTs and ILs is expected to produce a favorable support for the fabrication of metallic nanocatalysts [10].

In this work, as an example, PtPd alloy nanoparticles are electrochemically deposited on a multi-walled carbon nanotube (MWNT)–IL composite. The electrochemical oxidition of formaldehyde at the resulting composite film (i.e. PtPd–MWNT–IL) is explored, and it shows high electro-catalytic activity. When the PtPd–MWNT–IL composite coated glassy carbon electrode is used to sense formaldehyde, it presents wide linear range and good stability.

2. EXPERIMENTAL

2.1. Reagents

The multi-walled carbon nanotubes used (diameter: 10–30 nm, length: 0.5–40 μm, purity: ≥95%) came from Shenzhen Nanotech. Port Co. Ltd. (Shenzhen, China). The ionic liquid 1-octyl-3-methylimidazolium hexafluophosphate (OMIMPF$_6$, purity: 98%) was purchased from Acros Organics and used as received. H$_2$PtCl$_6$·6H$_2$O and PdCl$_2$·2H$_2$O were obtained from Sinopharm Group Chemical Reagent Co. (Shanghai, China). Formaldehyde was the product of Shanghai Zhanyun Chemical Co. Ltd. The working solutions were prepared by diluting the stock solution with H$_2$SO$_4$ solution and water. All other chemicals used were of analytical reagent grade, and the water used was redistilled.

2.2. Apparatus

Electrodeposition, cyclic voltammetric (CV) and chronoamperometric experiments were performed with a CHI 660 B electrochemical workstation (CH Instrument Company, USA). A conventional three-electrode system was adopted. The working electrode was a modified glassy carbon electrode or a glass substrate (10 mm×30 mm×2.2 mm) coated with a fluorine-doped tin oxide film (FTO: 150 nm, 20 Ω), and the auxiliary and reference electrodes were platinum wire and saturated calomel electrode (SCE), respectively. The scanning electron microscope (SEM) images were obtained using a Hitachi X-650 SEM (Hitachi Co., Japan), with an EDS meter for elemental chemical analysis. X-ray diffraction (XRD) data were recorded with a Rigaku D/max-rA diffractometer (Japan), using Cu Kα radiation (40 kV, 200 mA) with a Ni filter. All measurements were conducted at room temperature.

2.3. Preparation of composite film

The multi-walled carbon nanotube was purified through refluxing in HNO_3–H_2SO_4 (volume ratio: 1:1) mixture [11], washed with redistilled water and dried under vacuum. MWNT–OMIMPF$_6$/GCE was prepared as follows: 0.5 mg MWNT was dispersed in 1.0 mL redistilled water with the aid of ultrasonic agitation, and then 10.0 μL OMIMPF$_6$ was introduced in the mixture. Three microlitres of the resulting suspension was transferred on a cleaned glassy carbon electrode, and dried under an infrared lamp. The obtained electrode was noted as MWNT–OMIMPF$_6$/GCE. The electrodeposition was performed in 0.1 M, H_2SO_4 aqueous solution containing 1.0 mM H_2PtCl_6 and 1.0 mM $PdCl_2$. The electrodeposition potential was -0.28 V (*vs*. SCE) and the time was 400 s. The obtained PtPd–MWNT–IL/GCE was washed carefully with redistilled water and then dried at room temperature. Prior to electrodeposition, the solution was deoxygenated with nitrogen gas.

3. RESULTS AND DISCUSSION

3.1. Characterization of the composite film-coated electrode

Fig. 1 shows the XRD patterns of Pt, PtPd and Pd particles electrodeposited on FTO with MWNT–IL coating. They display a series of broad Bragg peaks, which are typical for materials of limited structural coherence. The peaks around 39.2, 45.4, 66.6 and 81.2° can be assigned to Pt (111), -(200), -(220), -(311) and -(222), respectively. And the peaks around 40.2, 46.4, 68.1 and 82.1° are assigned to Pd (111), -(200), -(220) and -(311), respectively. The XRD pattern of PtPd particles exhibits four major peaks, which shift to higher 2θ values (i.e. 39.7, 46.1, 67.7 and 81.6°) in comparison with those of Pt particles, indicating that the particles are alloy rather than a mixture of monometallic particles. The crystallite sizes (*d*) of Pt, PtPd and Pd particles are estimated according to the Scherrer equation [12], and they are 10.2 nm, 15.7 nm and 11.3 nm respectively. The percentage of Pt in the PtPd alloy is ca. 44.4% according to the EDS experimental result.

The SEMs of PtPd particles electrodeposited on bare FTO, MWNT/FTO and MWNT–IL/FTO are compared in Fig. 2. On the bare FTO, the obtained PtPd particles are big and the particle distribution is broad. On the MWNT/FTO, the PtPd particles are much smaller and they are more uniform. This is because MWNT provides many nucleation sites for PtPd formation [13]. For the MWNT–IL/FTO, the obtained PtPd particles are uniform and still smaller. This indicates that the IL also can promote the formation of small and uniform PtPd particles.

The influence of deposition time on the PtPd particles are tested (Fig. 2). When the electrodeposition time is 100 s, a few small PtPd alloy particles are deposited on the MWNT–IL/FTO. With increasing the electrodeposition time the particle density increases, and at about 400 s, the particle density reaches a maximum. When it exceeds 400 s the particle

density keeps almost unchanged, but the particle size increases gradually. For electrodeposition of 800 s, bigger PtPd clusters occur. When it is prolonged to 1200 s, the obtained particles agglomerate seriously. In the following experiments 400 s is selected.
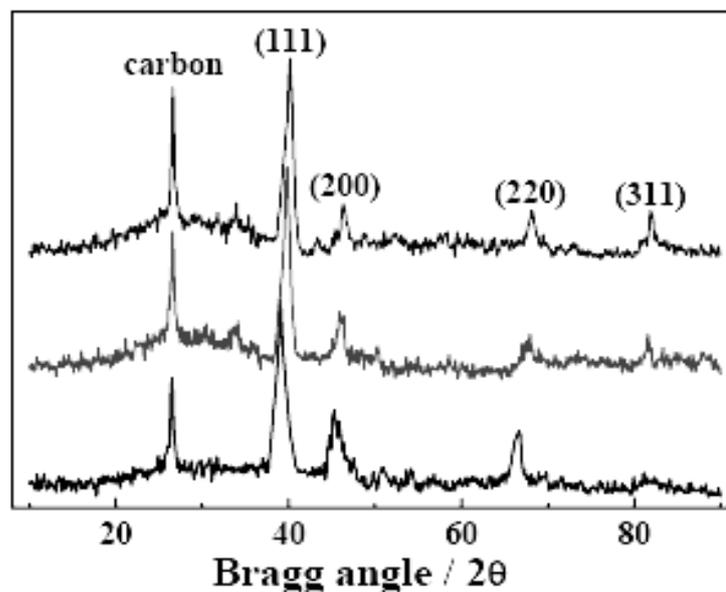

Fig. 1. XRD patterns of Pt, PtPd and Pd particles (from bottom to upper) deposited on MWNT–IL/FTO
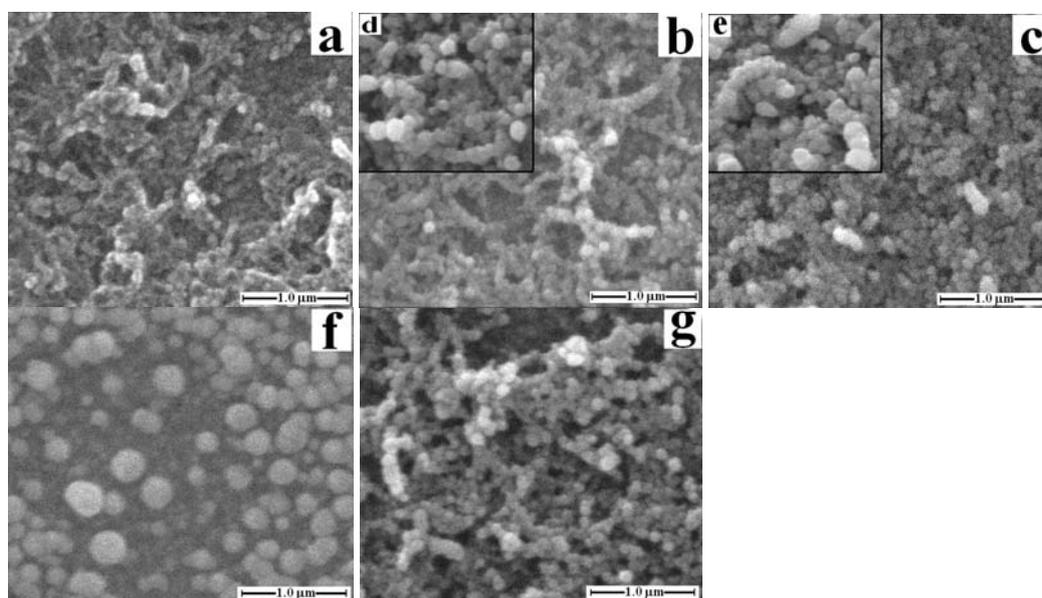

Fig. 2. SEM images of PtPd nanoparticles electrodeposited on MWNT–IL/FTO for 100 s, 200 s, 400 s, 800 s and 1200 s (a to e, their scales are same); SEM images of PtPd nanoparticles electrodeposited on bare FTO (f), MWNT/FTO (g) and MWNT–IL/FTO (c) for 400 s

The CVs of several electrodes in 0.2 M H_2SO_4 solution are recorded. The peaks characterizing the hydrogen adsorption/desorption and metallic oxide formation/stripping can be observed. For different electrodes the area of hydrogen adsorption/desorption peak follows the order of PtPd–MWNT–IL/GCE > PtPd–MWNT/GCE > PtPd/GCE. This is because more nanoparticles deposit on the MWNT–IL/GCE. On the other hand, the hydrogen adsorption/desorption peak area of PtPd/GCE is larger than that of Pt/GCE, implying that PtPd/GCE has bigger specific area or catalytic activity [14].

3.2. Electrocatalytic oxidation of formaldehyde at different electrodes

The cyclic voltammograms of Pt/GCE, Pd/GCE, PtPd/GCE, PtPd–MWNT/GCE and PtPd–MWNT–IL/GCE in formaldehyde solutions are shown in Fig.3(A). Formaldehyde exhibits three oxidation peaks. Among them two peaks are observed for the anodic sweep, while another peak occurs during the reverse sweep. The anodic peak at about 0.62 V can be attributed to the oxidation of CO_{ads} to CO_2 [15]. The peak at about 1.2 V may result from metal oxidation. During backward potential sweep, the peak at about 0.3 V can be ascribed to the oxidation of formaldehyde via a dehydrogenation reaction [16]. For different electrodes the peak area of the peak at 0.62 V follows such order as: PtPd–MWNT–IL/GCE > PtPd–MWNT/GCE > PtPd/GCE > Pt/GCE > Pd/GCE, indicating that the PtPd–MWNT–IL/GCE possesses larger active surface area. In addition, PtPd alloy nanoparticle may facilitate the decomposition of formaldehyde direct to CO_2, and thus suffers less influence from the product CO [15].

3.3. Influence of electrodeposition conditions on the electrocatalytic oxidation of formaldehyde

As can be seen in Fig. 3b, when the electrodeposition potential is -0.28 V, the peak of formaldehyde is bigger (take the peak at about 0.62 V for example). When the electrodeposition potential is more positive or more negative, the peak becomes smaller. This is mainly related to the alloy particle density or the electroactive area as the composition of the alloy keeps almost unchanged. At higher potential (e.g.: -0.20 V) the particle density is very low and the electroactive area is small. With potential decreasing, the particle density increases, so does the electroactive area. However, when it lowers to -0.30 V, particle agglomeration occurs. When the electrodeposition potential is -0.40 V, large PtPd nano-rods are obtained, the electroactive area is small. This may be due to the electrostatic repulse between electrode surface and $PtCl_6^{2-}$.

The electrodeposition time also shows great influence on the formaldehyde peaks. When the electrodeposition time is shorter (e.g.100 s or 200 s) the peak (at 0.62 V) is very small. When it is 400 s, the peak is sharper and higher. However, when it is 800 s and 1200 s, the peak becomes broad, while the peak current increases further.
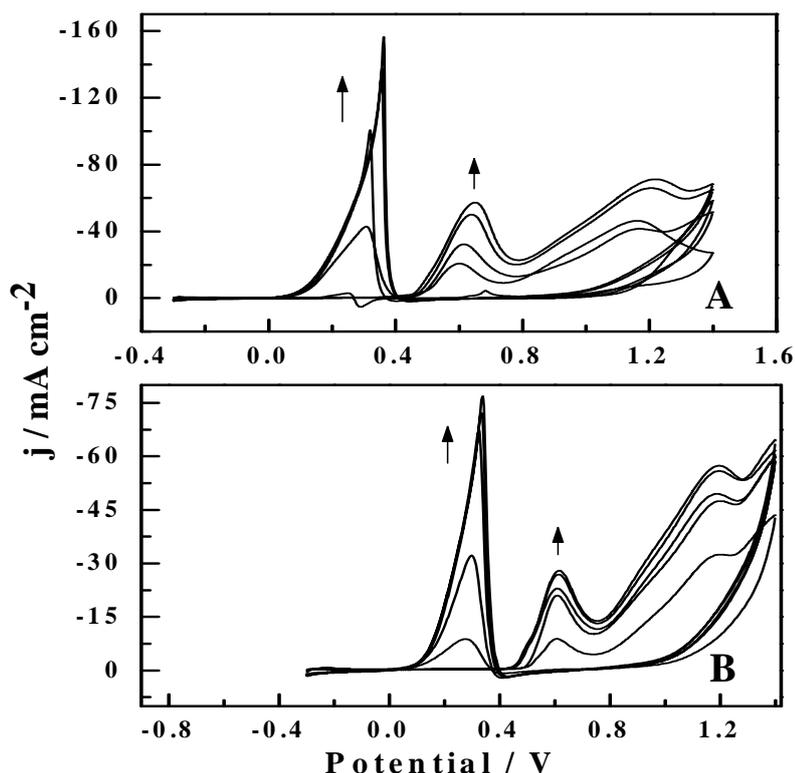
Fig. 3. (A) CVs of Pd/GCE, Pt/GCE, PtPd/GCE, PtPd–MWNT/GCE and PtPd–MWNT–IL/GCE (from inner to outer) in 0.2 M H_2SO_4 solution containing 0.20 M formaldehyde. **(B)** CVs of PtPd–MWNT–IL/GCE in 0.2 M H_2SO_4 solution containing 0.20 M formaldehyde. Electrodeposition potentials: -0.4 V, -0.2 V, -0.26 V, -0.3 V and -0.28 V (from inner to outer)

3.4. Influence of temperature on electrocatalytic oxidation of formaldehyde

Fig. 4 shows the amperometric response of PtPd–MWNT–IL/GCE to the addition of formaldehyde in stirred H_2SO_4 solution, and the relationship between the current and solution temperature. As can be seen, the current increases with temperature rising. Further more, it increases more rapidly at higher temperature. This is related to the change of diffusion rate and activated energy of formaldehyde; at higher temperature more formaldehyde molecules take part in the electrochemical reaction.

3.5. Chronoamperometric response and repeatability

Fig. 5 presents the current-time plots for formaldehyde. The response current is linear to formaldehyde concentration in the range of 2×10^{-4}–0.4 M, and the detection limit is about 1×10^{-5} M (S/N=3). In a formaldehyde solution, the response current density tends to stable value with time going, meaning that the PtPd nanoparticle has stable catalysis.

The repeatability of the PtPd–MWNT–IL/GCE is tested. A 0.2 M formaldehyde solution is detected with five electrodes prepared independently, and the relative standard deviation (RSD) of the respond current is 6.2%. Ten successive measurements using one electrode

yield an RSD of 3.6%. So the electrode is promising to be developed as a sensor for the detection of formaldehyde.
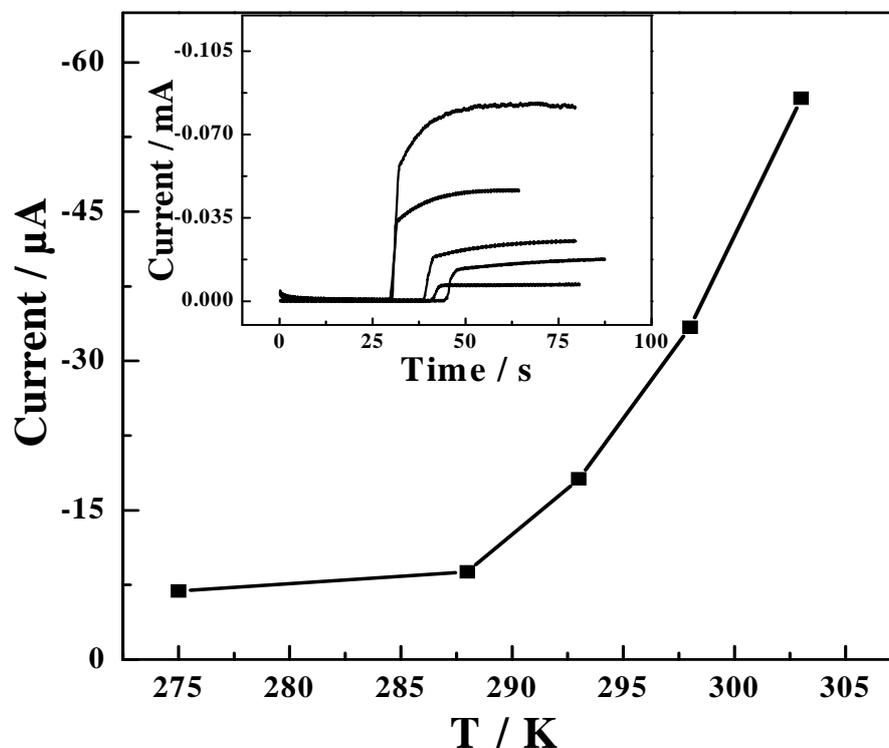

Fig. 4. The relationship between the response current and temperature; Inset: amperometric response of PtPd–MWNT–IL/GCE to the addition of 0.2 M formaldehyde to stirred 0.2 M H_2SO_4 solution; temperature: 275 K, 288K, 293 K, 298 K and 303 K (from bottom to upper); applied potential: 0.62 V
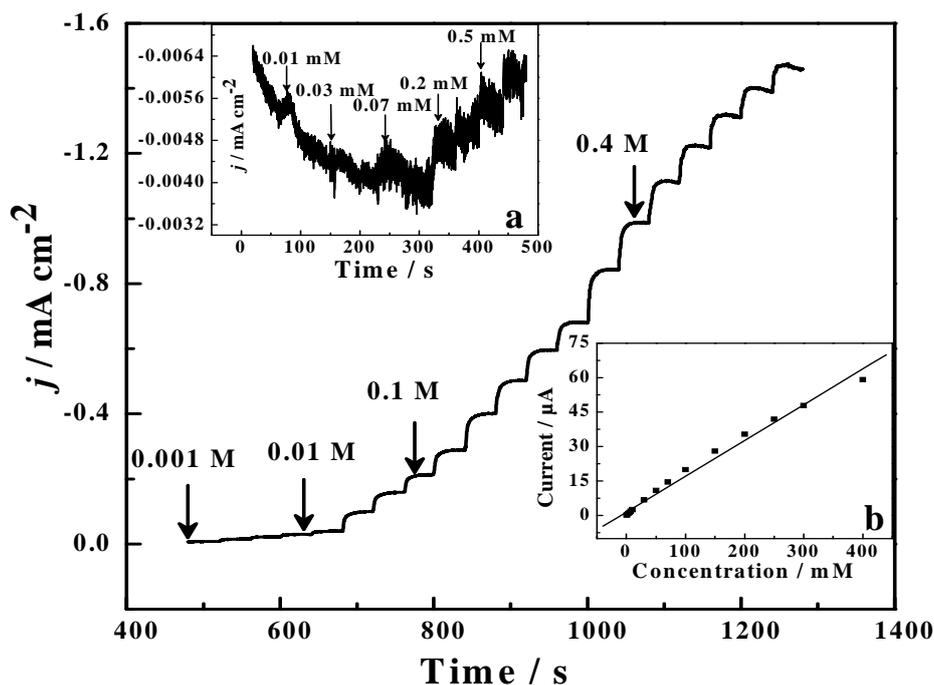
Fig. 5. Amperometric response of PtPd–MWNT–IL/GCE to successive addition of formaldehyde to 0.2 M H_2SO_4 solution. Applied potential: 0.62 V; insets: the amperometric response to the addition of 0.01, 0.03, 0.07, 0.2 and 0.5 mM formaldehyde (a); the calibration curve for the amperometric response of PtPd–MWNT–IL/GCE to formaldehyde (b)

4. CONCLUSION

Dense and uniform PtPd nanoparticle film can be electrodeposited on MWNT–IL coated GCE. The PtPd nanoparticles show feature of alloy. The obtained PtPd–MWNT–IL composite film has high catalytic activity to formaldehyde oxidation, and formaldehyde can exhibit large oxidation peaks at it. This opens a way for the preparation of metal nanoparticles based catalysts and sensors.

REFERENCES

[1] J. J. Huang, W. S. Hwang, Y. C. Weng, and T. C. Chou, Thin Solid Films 516 (2008) 5210.

[2] B. Liu, H. Y. Li, L. Die, X. H. Zhang, Z. Fan, and J. H. Chen, J. Power Sources 186 (2009) 62.

[3] E. Devers, C. Geantet, P. Afanasiev, M. Vrinat, M. Aouine, and J. L. Zotin, Applied Catalysis A 322 (2007)173.

[4] A. Safavi, N. Maleki, F. Farjami, and E. Farjami, J. Electroanal. Chem. 626 (2009) 75.

[5]   V. Ponec, and G. C. Bond (Eds.), Catalysis by Metals and Alloys, Elsevier, Amsterdam (1995).

[6]   G. Wu, Y. S. Chen, and B. Q. Xu, Electrochem. Commun. 7 (2005) 1237.

[7]   A. Safavi, N. Maleki, O. Moradlou, and M. Sorouri, Electrochem. Commun. 10 (2008) 420.

[8]   C.J. Jiang, H. Chen, C. Yu, S. Zhang, B. Hong, and J. L. Kong, Electrochim. Acta 54 (2009) 1134.

[9]   H. Itoh, K. Naka, and Y. Chujo. J. Am. Chem. Soc. 126 (2004) 3026.

[10] F. Xiao, F.Q. Zhao, J. J. Zeng, and B. Z. Zeng, Electrochem. Commun. 11 (2009) 1150.

[11] T. Fukushima, A. Kosaka, Y. Ishimura, T. Yamamoto, T. Takigawa, N. Ishii, and T. Aida, Science 300 (2003) 2072.

[12] V. Radmilovic, H. A. Gasteiger, and P. N. Ross, Catal. 154 (1995) 98.

[13] T. Fukushima, A. Kosaka, Y. Yamoto, T. Aimiya, S. Notazawa, T. Takigawa, T. Inabe, and T. Aida, Small 2 (2006) 554.

[14] J. T. Zhang, M. H. Huang, H. Y. Ma, F. Tian, W. Pan, and S. H. Chen, Electrochem. Commun. 9 (2007) 1298.

[15] V. Selvaraj, M. Alagar, and K. Sathish, Appl. Catal. B 75 (2007) 129.

[16] Z. Z. Zhu, Z. Wang, and H. L. Li, J. Power Sources 186 (2009) 339.